Supporting Information

K^+ intercalated MnO_2 with ultra-long cycling life for high-performance aqueous magnesium-ion hybrid supercapacitors

Liming Xu,[a#] Guodong Pan,[a#] Jiachen Wang,[a*] Jiabao Li,[b] Zhiwei Gong,[c] Ting Lu,[a*] Likun Pan[a*]

[a] *Shanghai Key Laboratory of Magnetic Resonance, School of Physics and Electronic Science, East China Normal University, Shanghai 200241, China*

[b] *School of Chemistry and Chemical Engineering, Yangzhou University, Yangzhou, Jiangsu 225002, China*

[b] *School of Physics and Electronic Science, East China Normal University, Shanghai 200241, China*

**Corresponding authors*

Email: lkpan@phy.ecnu.edu.cn (Likun Pan); jcwang@phy.ecnu.edu.cn (Jiachen Wang); tlu@phy.ecnu.edu.cn (Ting Lu)

[#] *Author Contributions: Liming Xu and Guodong Pan contributed equally*

Preparation of working electrode

80 wt.% active material, 10 wt.% Super P (conductive agent), and 10 wt.% polyvinylidene fluoride (binder) were mixed together in 1-methyl-2-pyrrolidone to form a homogeneous slurry. Then, the slurry was uniformly casted on graphite substrates (4 cm^2). Finally, the working electrode was dried in a blast drying oven at 60 °C for 48 h. The mass loading of active material on the working electrode is about 4 mg.

Electrochemical calculation

For the three-electrode and two-electrode systems, the specific capacitance (C_F, F g^{-1}; C, mAh g^{-1}) was calculated from the GCD curves according to the following equation [1,2,3]:

$$C_F = \frac{I \times \Delta t}{m \times \Delta V} \quad (1)$$

$$C = \frac{I \times \Delta t}{3.6 \times m} \quad (2)$$

where I, ΔV, m and v refer to the current (A), potential window (V), mass of active material (g) and scan rate (V s^{-1}), respectively.

For the two-electrode system, the energy density (E, Wh Kg^{-1}) and power density (P, W Kg^{-1}) were calculated according to the following equations [4,5]:

$$E = \frac{C_g \times \Delta V^2}{2 \times 3.6} \quad (3)$$

$$P = \frac{3600 \times E}{\Delta t} \quad (4)$$

where C_g, ΔV, and Δt refer to the specific capacitance (F g^{-1}), potential window (V), and scan rate (s), respectively.

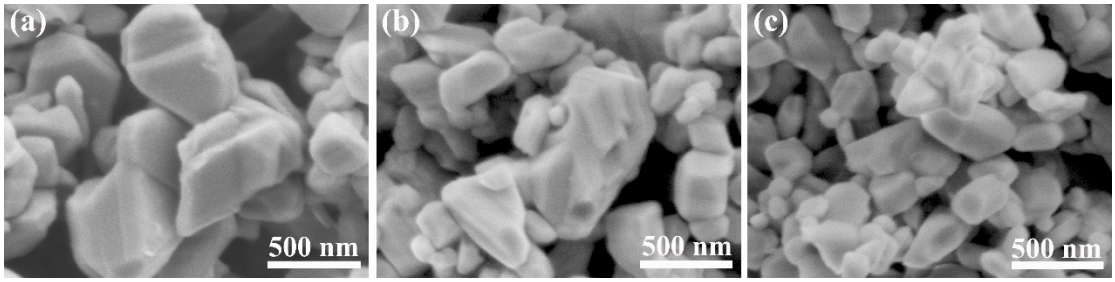

Fig. S1. SEM images of (a) K-MnO_2-1, (b) K-MnO_2-3, (c) K-MnO_2-4.

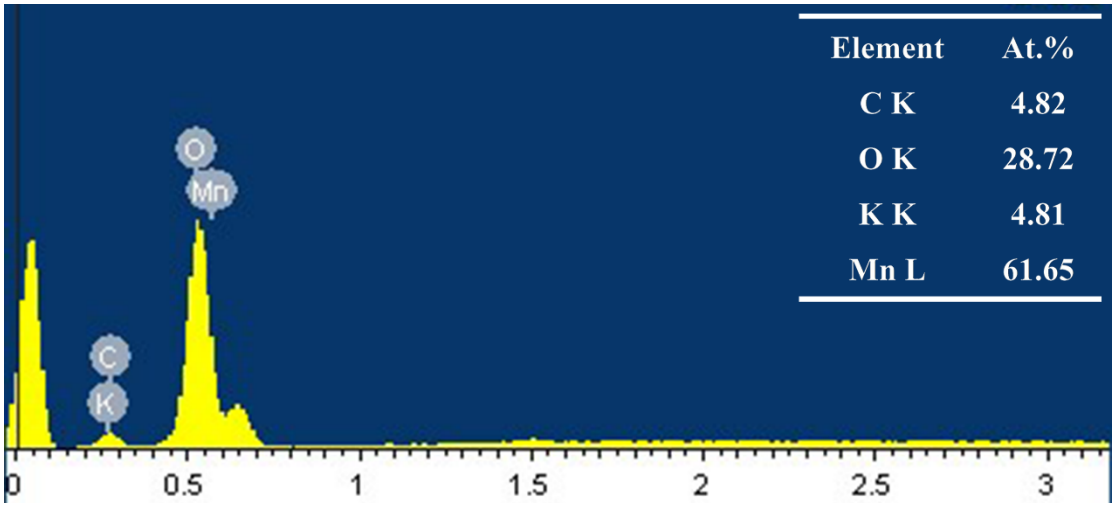

Fig. S2. Energy dispersive X-ray spectrum (EDS) analysis spectrum of K-MnO_2-2.

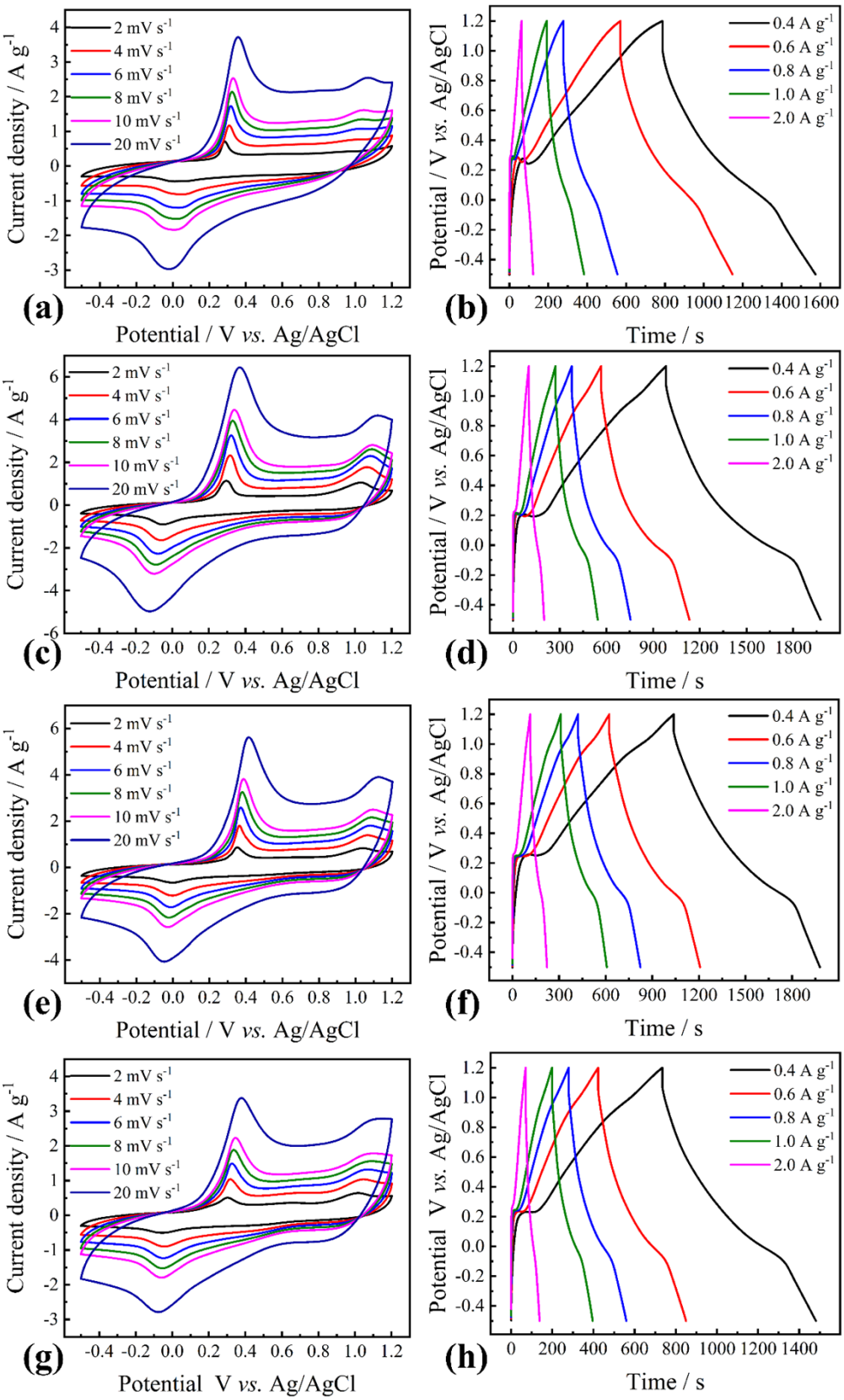

Fig. S3. CV curves at varied scan rates and GCD curves at different current densities of (a, b) MnO_2, (c, d) K-MnO_2-1, (e, f) K-MnO_2-3, and (g, h) K-MnO_2-4.

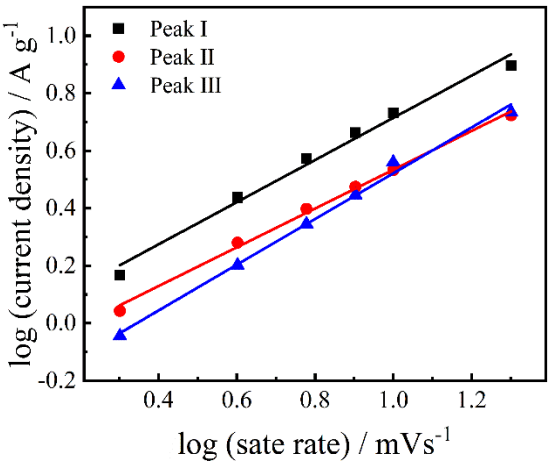

Fig. S4. Log(i)-Log(ν) curves of K-MnO_2-2.

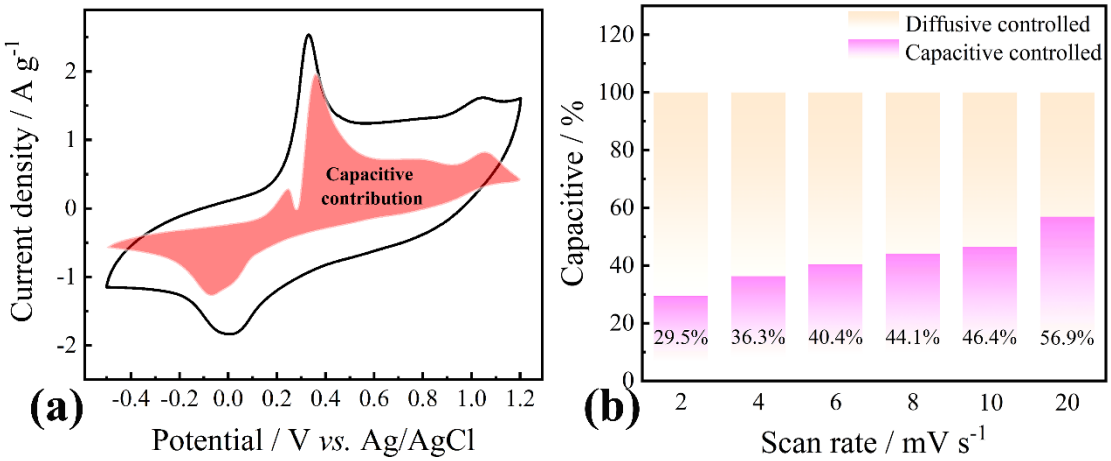

Fig. S5. (a) CV curve with the capacitive contribution at a scan rate of 10 mV s^{-1}, (b) the percentages of capacitive and diffusion contributions of MnO_2.

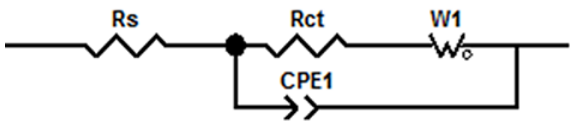

Fig. S6. Equivalent circuit diagram of MnO_2, K-MnO_2-1, K-MnO_2-2, K-MnO_2-3, and K-MnO_2-4.

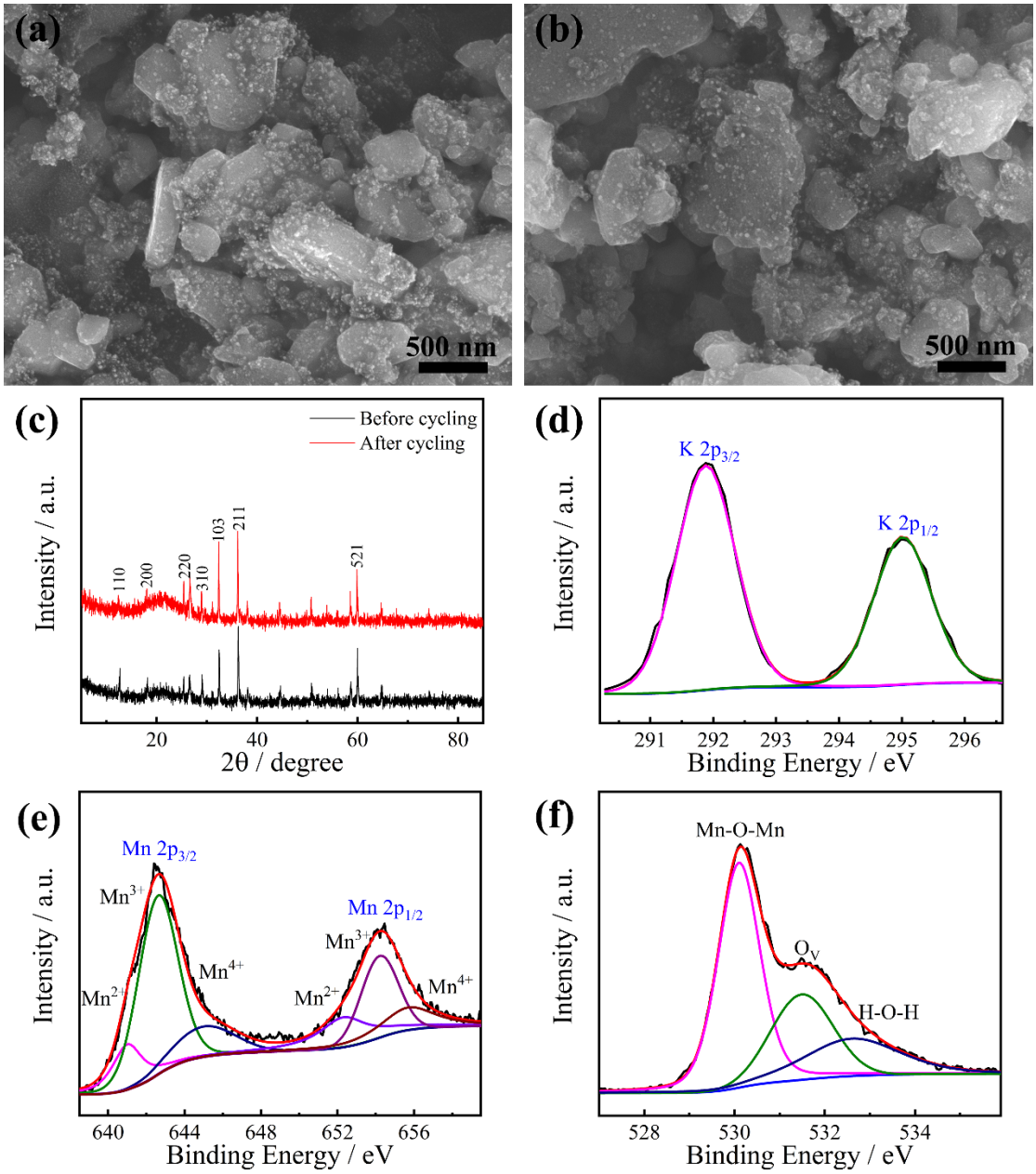

Fig. S7. SEM image of K-MnO_2-2 electrode before cycling (a) and after cycling (b). XRD patterns of K-MnO_2-2 electrode before and after cycling (c). XPS deconvolution of K 2p (d), Mn 2p (c), and O 1s (d) of the K-MnO_2-2 electrode after cycling.

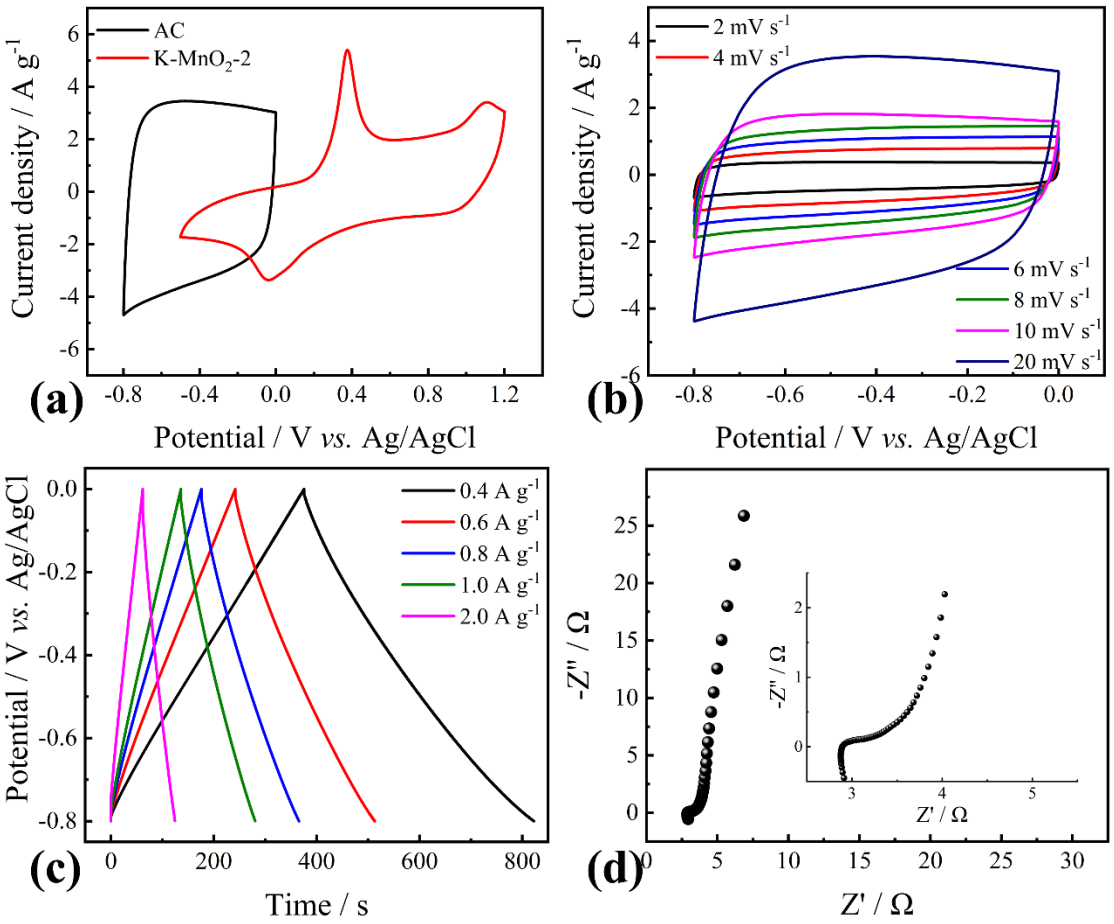

Fig. S8. (a) CV curves of AC and K-MnO_2-2 at a scan rate of 10 mV s^{-1}, (b) CV curves at 2-20 mV s^{-1}, (c) GCD curve at 0.5-2.0 A g^{-1}, and (d) Nyquist plots of AC (Inset shows the magnified plot in high-frequency region).

References

1 L.H. Wang, X.K. Ye, Y.C. Zhu, H.D. Jiang, J.X. Xia, Z.Y. Yue, Z.Q. Wan, C.Y. Jia and X.J. Yao, *Electrochim. Acta*, 2020, **340**, 135804.

2 L.M. Xu, D.H. Zhu, W.Q. Zhou, F.X. Jiang, Y.L. Wu, Y. Cai, H. Kang and J.K. Xu, *J. Energy Storage*, 2021, **43**, 103303.

3 N. Zarshad, A.U. Rahman, J.H. Wu, A. Ali, F. Raziq, L. Han, P. Wang, G.G. Li and H.M. Ni, *Chem. Eng. J.*, 2021, **415**, 128967.

4 J.W. Zhang, L.B. Zhu, H.T. Jia, K.X. Wei and L.X. Wen, *J. Alloys Compd.*, 2021, **889**, 161772.

5 L.M. Xu, Y.Y. Zhang, W.Q. Zhou, F.X. Jiang, H. Zhang, Q.L. Jiang, Y.H. Jia, R. Wang, A.Q. Liang, J.K. Xu and X.M. Duan, *ACS Appl. Mater. Interfaces 2020*, **12**, 45202-45213.